

# <sup>1</sup>H-NMR STUDY OF THE THREE LOW TEMPERATURE PHASES OF DPPC-WATER SYSTEMS

LUTZ TRAHMS, WOLF D. KLABE, AND EDWIN BOROSKE

*Freie Universität Berlin, Institut für Atom- und Festkörperphysik, Arnimallee 14, D-1000 Berlin 33, Federal Republic of Germany*

**ABSTRACT** The three phases of dipalmitoylphosphatidylcholine-water dispersions, occurring below the main transition are studied by a moment analysis of <sup>1</sup>H-nuclear magnetic resonance (NMR) spectra. The subtransition, recently detected by Chen, S. C., J. M. Sturtevant, and B. J. Gaffney, 1980, *Pro. Natl. Acad. Sci. USA*, 77:5060–5063, is characterized by a sharp drop in the second moment at 12°C as a result of increasing the temperature. Interesting features of this phase transition are a hysteresis of 11 K and extremely slow kinetics. It is interpreted as the onset of a flip-flop of the hydrocarbon chains about their long axis. At the pretransition, this type of motion is assumed to change into a fast rotation. The proposed models for the three phases are confirmed by computer calculations of theoretical values for the second and fourth moments of the corresponding NMR signals.

## INTRODUCTION

During recent years great efforts have been made to explore the phases and phase transitions of phosphatidylcholine-water dispersions. In particular dipalmitoylphosphatidylcholine (DPPC) was subjected to a large number of investigations, including x-ray (1, 2, 3) and neutron (4) scattering, electron microscopy (5), Raman spectroscopy (6, 7), electron spin resonance (8) and nuclear magnetic resonance (NMR) (9, 10, 11) studies. Today the liquid crystalline phase ( $L_\alpha$ ) that occurs above the main transition temperature at  $T_c = 42^\circ\text{C}$  is understood as a two-dimensional fluid with a lateral self-diffusion coefficient of  $2.6 \times 10^{-8} \text{ cm}^2\text{s}^{-1}$  (12). In a recent investigation (13) a further phase transition at even higher temperatures is discussed.

At lower temperatures there is still some uncertainty concerning dynamics and structure in the bilayer. Crystallographic studies have demonstrated the existence of a two-dimensional lattice of extended chains (14, 15) making an angle of  $10^\circ$  to  $15^\circ$  with the bilayer normal. The lattice was found to be hexagonal in the intermediate phase ( $P_\beta$ ) between 35 and  $41^\circ\text{C}$ , and slightly distorted (i.e., orthorhombic) in the gel phase ( $L_\beta$ ) at lower temperatures (16, 17, 18). A fascinating feature of the intermediate phase is the appearance of bilayer undulations (ripples) with wavelengths of  $\sim 200 \text{ \AA}$ , shown by x-ray (1, 2, 17, 18) and electron microscope (5, 19) studies. Other techniques, such as Raman (6, 7, 20) and NMR spectroscopy (21), could not provide further details about the long-range structure, but on the molecular scale dynamic changes at the pretransition from the gel to the intermediate phase became evident. As shown in the accompanying paper the correlation time,  $\tau_c$ , determined by proton-enhanced (PE)

<sup>13</sup>C-NMR experiments (22) drops by about one order of magnitude at the pretransition.

<sup>1</sup>H- and <sup>2</sup>H-NMR investigations by Davis (23) and MacKay (24) have confirmed that in the gel phase there is still a considerable amount of motion in the chain region of the bilayer. Both authors consider rotational motions about the long molecular axis a possible interpretation. A disordered segmental motion of the chains was excluded by infrared studies of Cameron et al. (25, 26). These studies show clearly that in the gel phase the chains are extended with no substantial average population of gauche conformers. Interestingly, both Davis (23) and Cameron et al. (27) found that the chain motion disappears below  $0^\circ\text{C}$ .

Recently Chen et al. (28) detected a third-phase transition in DPPC liposomes between 10 and  $20^\circ\text{C}$  by means of differential scanning calorimetry (DSC). The latent heat and width of this so-called subtransition depended on the history of their samples. The precise transition temperature,  $T_s$ , could not be determined from their data because apparently in all experiments the transition was too slow to permit immediate equilibration at the slowest possible speed of DSC. The nature of this subtransition is the main subject of this paper. As far as temperatures above  $12^\circ\text{C}$  are concerned, our data are in good agreement with similar measurements of MacKay (24), whereas in contrast to his results below this temperature, we observe strong evidence of the subtransition. Referring to the results of Chen et al. (28), we attribute this discrepancy to differences in the history of the sample.

As an extension of the nomenclature introduced by Tardieu et al. (1) we will refer to the phase below the subtransition as  $L_s$  in this article. Both, the Letter  $L$  (indicating that there is no periodicity in the plane of the

lamellae) and the prime (indicating that the chains still form a tilt angle with the normal of the lamellae) seem to be justified from the available x-ray results, although unambiguous experimental proof is still necessary. In this study  $^1\text{H}$ -NMR is shown to be a most sensitive method for detecting dynamic changes in the low temperature phases of DPPC-water systems. On the basis of our results we propose a model that involves the onset of rotational chain dynamics at the subtransition. This dynamic information may be regarded as a supplement to the structural data reported in recent x-ray studies (29, 30).

## MATERIALS AND METHODS

A detailed description of the preparation of the DPPC- $\text{D}_2\text{O}$  dispersions is given in the accompanying paper (22). Note that before starting a set of measurements we kept the sample at  $0^\circ\text{C}$  for at least two days. If this procedure was not followed few if any subtransition effects were observed. Longer cooling periods had no further effects on the experimental results. NMR-experiments were performed on a SXP 4-100-MHz spectrometer (Bruker GmbH, Karlsruhe, FRG) operating at 80 MHz. The free-induction decay (FID) data were acquired by a transient digitizer B-C 104 (Bruker GmbH) in connection with a HP 21 MX real-time computer system. Averaging and data storage procedures were carried out with homemade software. In case of the spin-pair dipolar-echo (SPDE) experiments, the noise reduction of the echo amplitude was performed by a boxcar integrator with time resolution of  $2\ \mu\text{s}$ . Owing to the  $8\text{-}\mu\text{s}$  dead time of the receiver, both the FID and the SPDE had to be extrapolated to  $t = 0$  by a Gaussian fit.

## THEORY

Compared with other sophisticated NMR techniques, such as proton-decoupled  $^{13}\text{C}$ -NMR, the  $^1\text{H}$ -FID of disoriented multilamellar DPPC- $\text{D}_2\text{O}$  dispersions contains only few details. A well established theoretical approach to describe these broadline spectra is the method of moments. In this formalism the FID of the transverse magnetization of a homogeneous spin reservoir following a  $90^\circ$  radio frequency pulse is described by a series expansion (31)

$$G(t) = 1 - \frac{1}{2!} M_2 t^2 + \frac{1}{4!} M_4 t^4 - \dots, \quad (1)$$

where  $M_2$ ,  $M_4$ , etc., represent the even moments of the corresponding continuous-wave (cw) resonance line. In the case of  $^1\text{H}$ -NMR in a rigid lattice the first two moments are given by (32)

$$M_2 = \frac{1}{4} \gamma^4 \hbar^2 \sum_k b_{jk}^2 \quad (2a)$$

$$M_4 = 3 M_2^2 - \frac{\gamma^8 \hbar^4}{8} \left[ \frac{1}{6N} \sum_{j \neq k} b_{jk}^2 (b_{ji} - b_{ki})^2 + \sum_k b_{jk}^4 \right], \quad (2b)$$

where  $\gamma$  is the gyromagnetic ratio of the proton,  $N$  is the number of interacting spins, and  $b_{jk}$  represents the dipolar-interaction terms given by

$$b_{jk} = \frac{3}{2} \frac{1 - 3 \cos^2 \theta_{jk}}{r_{jk}^3} \quad (3)$$

with the vector  $r_{jk}$  connecting the two spins forming an angle  $\theta_{jk}$  with the applied external magnetic field,  $H_0$ .

These expressions were derived under the assumption that spin  $j$  is representative for each spin of the sample, i.e., the spins form a homogeneous spin reservoir. It has been established, however, that in DPPC- $\text{D}_2\text{O}$  dispersions at least two molecular spin reservoirs have to be distinguished: the hydrocarbon chains and the head-group moiety (21). The major contribution of the head-group protons can be subtracted from the total magnetization decay to analyze the chain signal separately. Owing to the strong dipolar coupling, the protons of an extended chain can be considered as a homogeneous spin reservoir (with some modifications discussed below) and Eqs. 2a and b apply to this part of the molecule.

The ratio of moments  $R = M_4/M_2^2$  provides some information about the shape of the magnetization decay and its Fourier transform, the corresponding cw-absorption resonance line. With  $R = 3$  the first three terms in Eq. 1 represent a Gaussian expansion, and the observable part of both FID and the cw-resonance line can be fitted by a Gaussian shape. A smaller value of  $R$  results in a flattening of the top of the cw-resonance line or even a splitting into two lines. In pulsed NMR this corresponds to an oscillatory behavior of the FID. A detailed elaboration of this relation requires taking into account the higher moments  $M_6$ ,  $M_8$ , etc., which would become very cumbersome because of the complexity of the expressions for the higher moments. It appears that the method of moments is not the appropriate formalism for  $R \ll 3$ .

From Eq. 2b it is evident that for a homogeneous spin reservoir a deviation of  $R$  in the other direction, i.e.,  $R > 3$  is impossible. Only the simultaneous existence of different spin reservoirs with diverging second moments can give rise to a ratio of moments higher than 3. In that case the result is a narrowing of the cw-resonance line becoming Lorentzian-like rather than Gaussian. The corresponding FID would be close to an exponential decay. A more detailed discussion of this point is given in reference 33.

In the systems considered here thermal motions of the molecules reduce the dipolar interaction between the spins. In Eqs. 2a and b therefore  $b_{jk}$  has to be replaced by  $\langle b_{jk} \rangle$ , the average dipolar interaction during the observation time. In the liquid crystalline  $L_\alpha$  phase, where fast formation of gauche conformations and kinks occur in many positions of the chain, the appropriate method to describe the averaging process is given by the order parameter

$$S_{jk} = \frac{1}{2} \left\langle 3 \cos^2 \theta_{jk} - 1 \right\rangle. \quad (4)$$

At lower temperatures, where the chains are assumed to be in all-*trans* conformation, other dynamic models have to be discussed.

In earlier studies (34-37) it was established that in samples containing spin-1/2 pairs, such as the methylene

protons of hydrocarbon chains, part of the decay of the transverse magnetization can be reversed by applying a second  $90^\circ$ -pulse that is shifted in phase by  $90^\circ$ . This refocusing is due to the dipolar interaction within the spin pairs. The height of the maximum echo amplitude therefore is determined solely by the interpair interactions. In terms of the moments the quantity derived from the spin-pair dipolar-echo decay is  $M_{n \text{ interpair}}$ , given by Eqs. 2a and b, when all intrapair interaction terms (Eq. 3) are omitted.

## RESULTS AND DISCUSSION

### Entire Molecule

Fig. 1 presents linearized plots of four FID's, each representing one of the four observed phases. The corresponding SPDE decays are shown in Fig. 2. Each plot exhibits a

superposition of at least two Gaussian-shaped decays, a result of the molecular inhomogeneity of the proton-spin reservoir discussed above. Other types of inhomogeneities within the sample were ruled out by a number of additional experiments. (a) Samples with varying water content (25–60%) exhibit similar  $^1\text{H}$ -NMR lineshapes (38). (b) FID and SPDE decays of compounds with a deuterated choline moiety exhibit single, Gaussian-like decays (38). (c) PE- $^{13}\text{C}$  spectra do not show any evidence of inhomogeneities within the sample (22).

Therefore the fast part of the decay is due to the apolar region of the molecule including the 5 glycerol protons, which are in a configuration similar to the all-*trans* arrangement of the hydrocarbon chains. In the gel and intermediate phase this part amounts to some 85% of the total signal. In this state the magnetization of all choline protons decays with a substantially slower time constant as

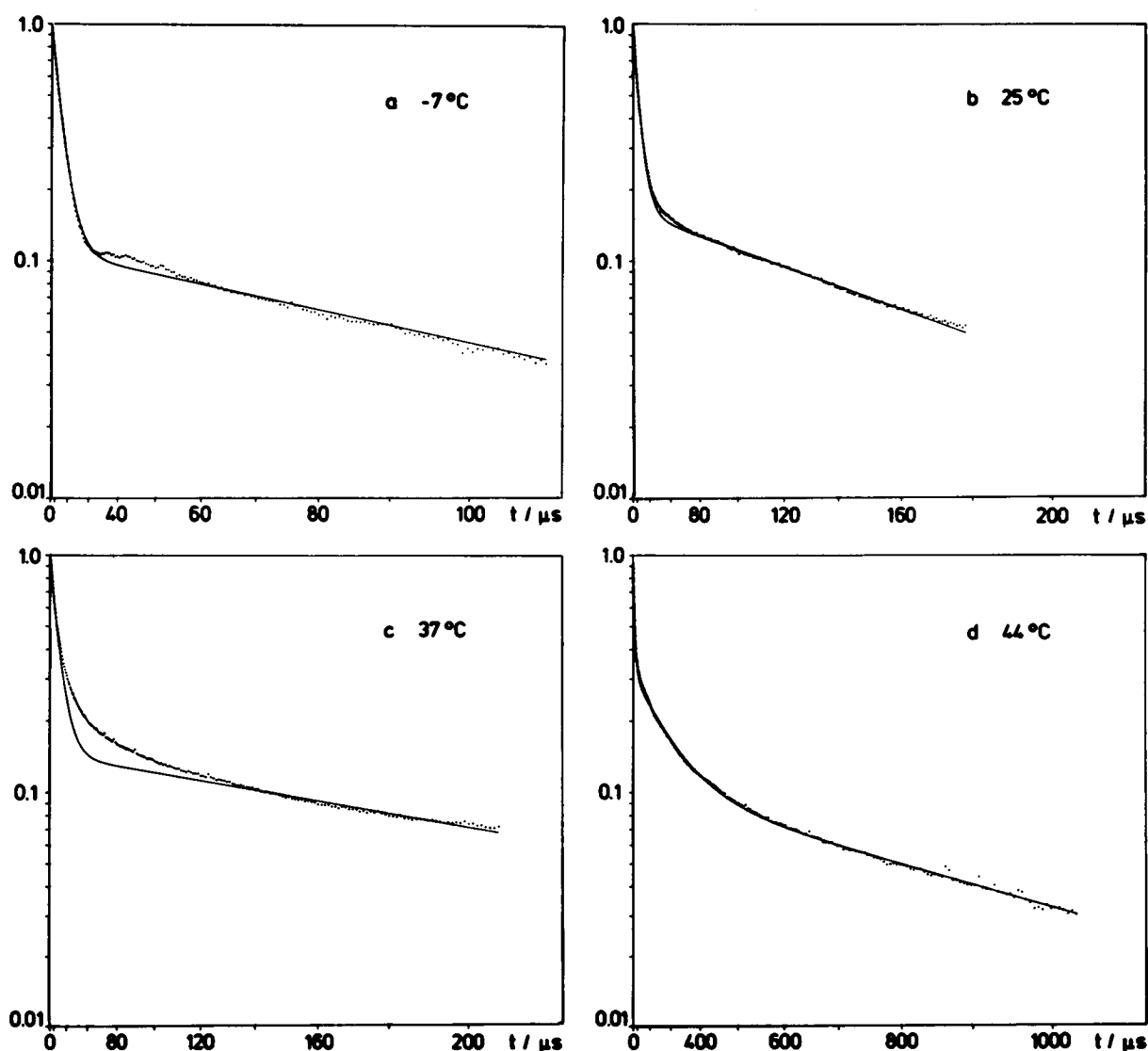


FIGURE 1 Four plots of free-induction decays (FID's), each one (a–d) representing one of the four observed phases. The drawn lines are least-square fits to a superposition of two or, in case of the fluid  $L_\alpha$  phase in d, three Gaussian decays.

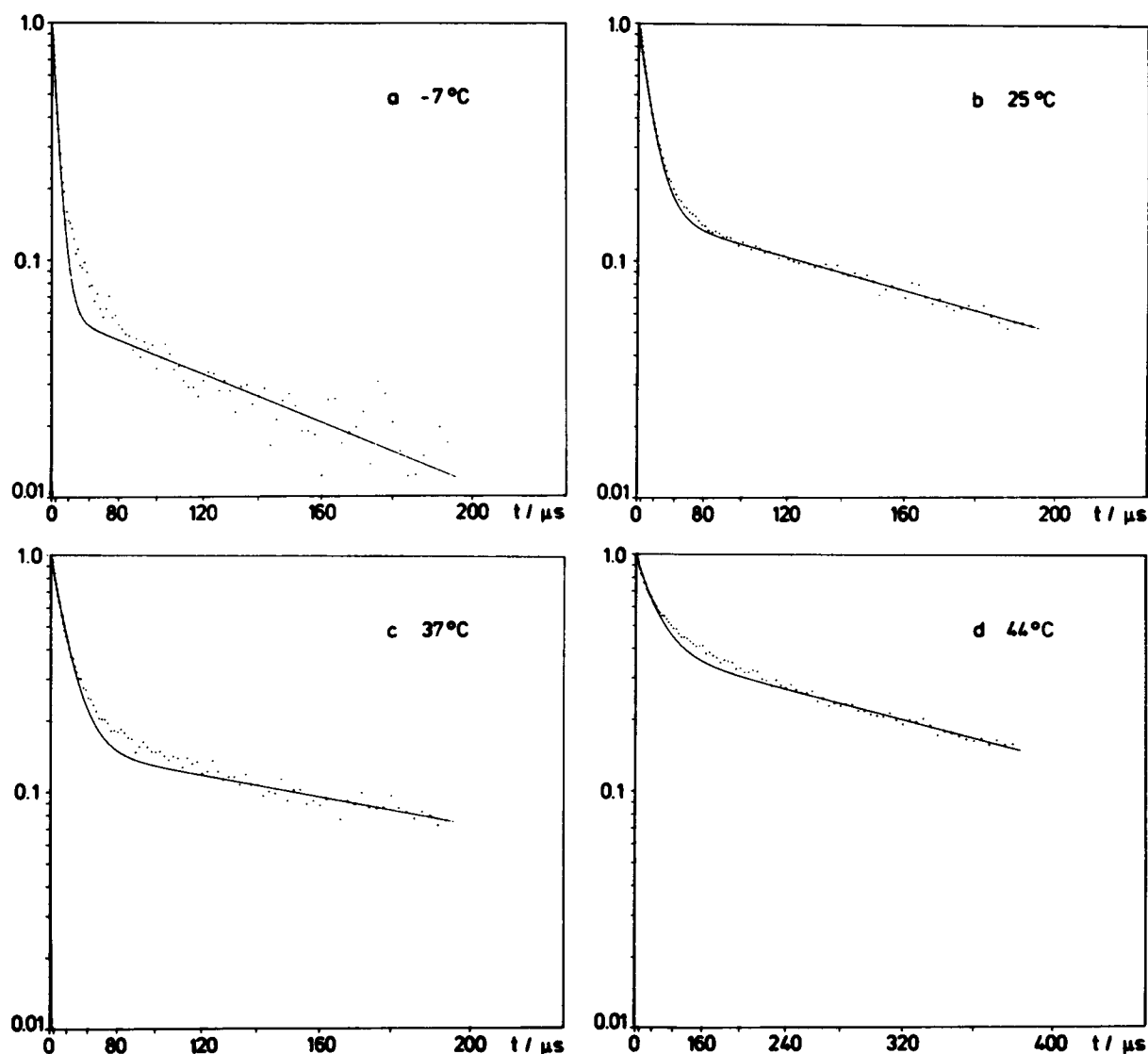


FIGURE 2 Four plots of spin-pair dipolar-echo decays, each one (a-d) representing one of the four observed phases. The drawn lines are least-square fits to a superposition of two Gaussian decays.

the result of motional narrowing caused by a number of intramolecular rotations (10, 39, 40). For our purposes we shall divide the rotations into two classes: (a) rotations that affect only the 9 methyl protons, i.e., the rotation of the 3 methyl groups about the N-(CH<sub>3</sub>)<sub>3</sub> bonds and the rotation of the entire N-(CH<sub>3</sub>)<sub>3</sub> group about the CH<sub>2</sub>-N bond ( $\alpha_6$  and  $\alpha_7$  in the nomenclature of Seelig [41]); and (b) rotations that affect the entire choline head group ( $\theta_1$ ,  $\alpha_1 - \alpha_5$ ), such as the rotation about the P-O bond to the glycerol moiety ( $\alpha_2$ ).

It is well known that in the liquid crystalline  $L_\alpha$  phase disordered kinks are rapidly formed along the hydrocarbon chains. A decrease in both the segmental order parameter (9, 42) and the rotational correlation time (43) towards the chain end was found in earlier investigations. Kink formation thus gives rise to a motional narrowing of the <sup>1</sup>H linewidth, which is inhomogeneously distributed along the

hydrocarbon chain. Moreover, the second moment of a chain undergoing fast rotation is strongly dependent on the angle of its long axis with the external field, as shown below. It is no surprise, therefore, that the decays observed in the  $L_\alpha$  phase cannot be fitted by a superposition of two Gaussian decays.

At low temperatures, i.e., below the subtransition, the lineshape changes drastically. The relative amount of the slow decay drops to some 10% indicating that part of the choline protons have stopped their rapid motion and thus exhibit a second moment similar to that of the chains. The view that fast rotations that affect the entire choline head group are absent below the subtransition is supported by the incomplete motional averaging of the <sup>31</sup>P-shift tensor observed by Földner in a recent study (29). Another feature of the low temperature <sup>1</sup>H-FID is the slight oscillatory character of the chain signal. This aspect shall

be discussed below in the lineshape analysis of the chain signal.

Because of experimental errors in the baseline of the spectrometer and the presence of ~1%  $^1\text{H}$  in the heavy water, it is extremely difficult to obtain reliable data for  $M_2$  of the choline moiety. In the following section we want to restrict our moment analysis to the apolar part of the

DPPC molecule, whose moments are mainly determined by the moment of the hydrocarbon chains.

### Hydrocarbon Chain

The data for  $M_2$  (chain) (Fig. 3) were derived from the observed decays by a double Gaussian fit, indicated by the drawn lines in Figs. 1 and 2. The experimental errors in the second moments are below 5%. Four phases of the DPPC-water dispersions are separated by steps in the plots of  $M_{2\text{ total}}$  (chain) and  $M_{2\text{ interpair}}$  (chain) vs. temperature: the well-known liquid crystalline  $L_\alpha$  phase, the  $P_\beta$  (intermediate) phase, the  $L_\beta$  (gel) phase, and, by a surprisingly sharp drop, a fourth low temperature phase that is identified as the recently detected  $L_\alpha'$  phase below the subtransition (28, 29, 30). An interesting feature of this transition is the hysteresis of 11 K that was found to last at least several days.

An example of the kinetics of the subtransition is demonstrated in Fig. 4. At temperatures slightly above the transition temperature of 12°C, the adjustment of the gel phase occurs extremely slowly, whereas at higher temperatures the kinetics are considerably faster. Presumably this is the reason why there was some uncertainty about the precise transition temperature in the calorimetric study of Chen et al. (28). Even slower kinetics were observed when the temperature was decreased to near 1°C.

Basically two features of our data need to be interpreted in terms of geometrical arrangement and motional behavior of the chains in the bilayer (a) the function  $M_2(T)$ , and (b) the lineshapes of FID's and SPDE decays. The first approach to understanding the sharp drop of the second moment at  $T_s$  is to assume the onset of some kind of motion of the hydrocarbon chains around their long axis. It is well known that a free rotation around a single axis with a correlation time,  $\tau \ll M_2^{-1/2}$ , causes a significant reduction of the second moment by motional averaging. In particu-

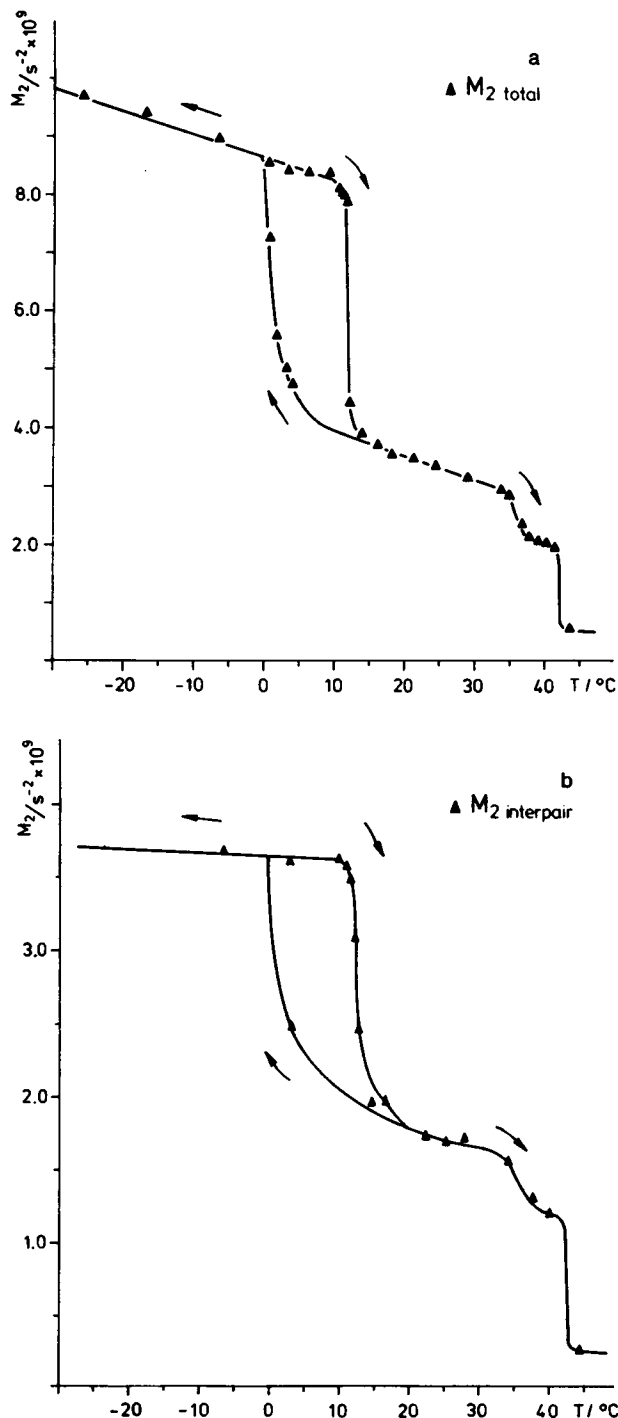


FIGURE 3 Temperature dependence of the observed second moments (a)  $M_{2\text{ total}}$  and (b)  $M_{2\text{ interpair}}$  of the hydrocarbon chains.

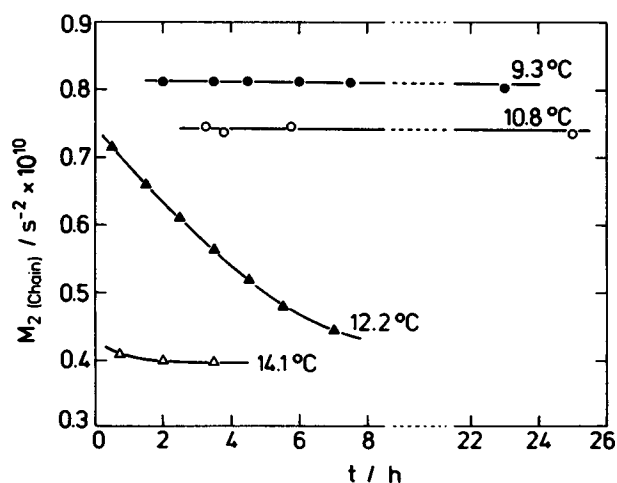


FIGURE 4 Time dependence of the phase transition around 12°C with increasing temperature.

lar, for two spins of one chain the term  $1 - 3 \cos^2 \theta$  in Eq. 3 transforms into

$$(1 - 3 \cos^2 \theta)_{\text{rot}} = \frac{1}{2}(1 - 3 \cos^2 \theta') (3 \cos^2 \gamma - 1), \quad (5)$$

where  $\theta'$  and  $\gamma$  are the angles of the long-chain axis with the applied external field,  $H_0$ , and the connecting vector  $\mathbf{r}_{jk}$ , respectively. In the case of two neighboring methylene protons, where  $\gamma = 90^\circ$ , the resulting reduction factor for a polycrystalline sample is exactly 4. In fact the intramethylene second moment derived from Figs. 3 a and b,

$$M_{2 \text{ intra}} = M_{2 \text{ total}} - M_{2 \text{ inter}}, \quad (6)$$

decreases from  $4.7 \times 10^9 \text{ s}^{-2}$  at  $T < T_s$  to  $1.0 \times 10^9 \text{ s}^{-2}$  in the intermediate phase below the main transition, which yields a factor of 4.7. So far this interpretation gives a rough picture of the two extreme ends of the low temperature range: more or less immobile chains in the  $L_\sigma$  phase and free or hindered rotations with  $\tau_c < M_2^{-1/2}$  about the chain axis in the  $P_\beta$  phase.

A more detailed model can be worked out considering some crystallographic data. According to x-ray results of Hentschel (17) the packing of the hydrocarbon chains (demonstrated in Fig. 5) changes from hexagonal with a ratio  $a/b = 1.73$  in the intermediate phase to orthorhombic with  $a/b = 1.69$  below the pretransition. The data of Földner (44) yield  $a/b = 1.44$  for the  $L_\sigma$  phase. Within the experimental errors this value is consistent with the paraffin ratio,  $a/b = 1.49$ . The sharp drop in the chain-packing density at the subtransition is likely to coincide with the onset of some kind of chain motion around their long axis. The model suggested here for the gel phase is a correlated disrotatory oscillation between the two equivalent configurations as shown in Fig. 5.

On the basis of these crystallographic data we have calculated the theoretical values of the second and fourth moments corresponding to the following models: (a) the  $P_\beta$  phase, hexagonal lattice with fast rotating chains; (b) the  $L_\beta$  phase, orthorhombic lattice with a  $90^\circ$  flip-flop of the chains; and (c) the  $L_\sigma$  phase, paraffin lattice with rigid chains. They hydrocarbon chains were assumed to be in an all-*trans* conformation with C—C and C—H distances of 1.54 and 1.09 Å, respectively, and binding angles C—C—C and H—C—H of  $111^\circ$  and  $109^\circ$  (44), respectively. Note that in these computations it is assumed that all spins in the chain are equivalent, neglecting boundary effects at both ends of the chain. Also the two protons of a methylene

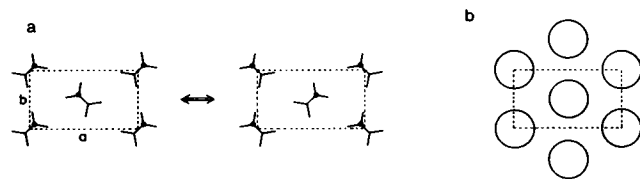


FIGURE 5 Two dimensional hydrocarbon lattice of the lecithin bilayer (a) orthorhombic ( $L_\beta$ ) and, (b) hexagonal ( $P_\beta$ ).

group in an orthorhombic lattice are not in equivalent positions, leading to diverging results in the interchain second moments. We assumed a value equal to the average of the two.

The results for  $M_2$  given in Table I are in good agreement with those obtained by other authors (45, 46, 47). In our computation we have distinguished between the intra- and interpair contributions to  $M_{2 \text{ total}}$ . The polycrystalline averaging was done numerically varying the magnetic-field vector in small steps ( $< 5^\circ$ ) uniformly in all directions. This effort would not have been necessary for the mere calculation of  $M_2$ , where the spatial averaging leads to

$$\left\langle (1 - 3 \cos^2 \theta)^2 \right\rangle = \frac{4}{5}. \quad (7)$$

Thus this term can be taken outside the summation in Eq. 2a. But as made evident by Eq. 2b this procedure does not apply to the fourth moment. This has some implications concerning the lineshape of the observed polycrystalline sample as discussed in the next section. As for the second moments this cumbersome procedure leads to the same results as those obtained by the simpler calculation according to Eq. 7 within 0.1% tolerance.

The results are listed in Table I in comparison with the experimental findings. In all phases the calculated values of  $M_{2 \text{ total}}$  and  $M_{2 \text{ inter}}$  are about two times larger than the experimental values. Such discrepancies were already observed by other authors for soaps (46, 47) and DPPC (24, 48) and can be explained in part by boundary effects (46), but obviously the main source of the reduction in the observed residual second moment lies in intrachain dynamics. The calculations were carried out without considering any kind of vibrational motion within the chain, such as e.g., small torsions of the segments around the long-chain axis (24). The negative slope in each phase of the function  $M_2(T)$  indicates the existence of a degree of motional freedom, which reduces the dipolar broadening. Still other types of motion may cause narrowing in the observed spectra. As discussed in the preceding paper we doubt, however, that fast lateral molecular diffusion within the two-dimensional lattice, which is confirmed by many x-ray studies for all phases below the main transition (14–18), is sufficient for the observed dipolar-line narrowing.

Considering the relative changes in  $M_2(T)$ , however, the theoretical calculations are in good agreement with the experimental data. This confirmation of the suggested model finds further corroboration in the theoretical computation of the ratio of moments,  $R = M_4/M_2^2$ . As pointed out above, this parameter provides some information about the shape of the decays. The cumbersome calculation of  $R$  has been carried out for the case of rigid ( $L_\sigma$  phase) and fast rotating chains ( $P_\beta$  phase). In the latter case interchain interactions were neglected. The results for the subphase is  $R = 2.5$ . There is indeed some qualitative

TABLE I  
COMPARISON OF CALCULATED AND MEASURED VALUES OF THE SECOND MOMENTS OF THE  
HYDROCARBON  
CHAINS IN A POLYCRYSTALLINE SAMPLE FOR THE THREE LOW TEMPERATURE PHASES\*

	Theoretical		Experimental		
	$M_{2 \text{ total}}$	$M_{2 \text{ interpair}}$	$M_{2 \text{ total}}$	$M_{2 \text{ interpair}}$	
Rigid lattice $a = 7.80 \text{ \AA}$ $b = 5.33 \text{ \AA}$	16.6	8.5	8.4	3.7	$T = 7^\circ\text{C}$ (subphase)
90° flip-flop $a = 8.14 \text{ \AA}$ $b = 4.86 \text{ \AA}$	6.2	4.1	2.9	1.7	$T = 32^\circ\text{C}$ (gel phase)
Rotation $a = 8.36 \text{ \AA}$ $b = 4.86 \text{ \AA}$	5.2	3.1	2.2	1.2	$T = 38^\circ\text{C}$ (intermediate phase)

\*All data are given in  $\text{s}^{-2} \cdot 10^9$ .

experimental evidence for this low value of  $R$  in our data: the FID's recorded in the  $L_\sigma$  phase (Fig. 1 *a*) show a slight oscillatory behavior.

An interesting problem arises from the computational result for the intermediate phase,  $R = 4.8$ . The corresponding experimental evidence for  $R > 3$  is found in the deviation of the FID from a double Gaussian fit as illustrated in Fig. 1 *c*. Similar experimental features were observed by MacKay (24), who derived  $R$  by integration of the Fourier transform of the FID. His data yield an increase in  $R$  from 3.0 to 4.0 at the pretransition, which is consistent with both our qualitative observation and quantitative theoretical calculation.

At first sight a value of  $R$  larger than 3 seems to imply the existence of inhomogeneities in the sample. This model calculation, however, shows that  $R > 3$  is solely produced by the angular dependence of  $M_2$  of a fast rotating chain. In this case the values of  $M_2$  and  $M_4$  vary in a wide range from a maximum of  $M_2 = 5.5 \times 10^9 \text{ s}^{-2}$  for  $\theta = 90^\circ$  to zero at the magic angle, but the ratio of moments remains constant at  $R = 2.24$ . Thus the resulting FID is a superposition of decays with very different second and fourth moments, and the inhomogeneities are simulated by the simultaneous observation of many fast rotating chains with a uniform angular distribution with respect to the external magnetic field. Thus the observation of a polycrystalline sample yields a ratio of moments  $R > 3$ , instead of  $R = 2.24$  for any single field direction.

## CONCLUSION

In spite of the lack of spectral details the  $^1\text{H}$ -NMR data of this study allow some insight into dynamics and crystalline structure of DPPC bilayers. The conclusions from this investigation can be summarized as follows. (*a*) Below the subtransition any kind of rotational motion in a time domain accessible to  $^1\text{H}$ -NMR ceases. Other kinds of motion are likely to be still present, such as torsion in the

C—C bonds of the chains around the long axis. It is plausible that a change in chain packing accompanies the freezing of rotational motion. Also the fast rotation of the entire choline head group disappears, whereas the fast rotation of the  $\text{N}(\text{CH}_3)_3$  group is still present. This finding suggests a superlattice of the head groups aligned in the bilayer plane by electric interactions between the  $\text{P}^--\text{N}^+$  dipoles. (*b*) Spectral changes at the subtransition to the gel phase are explained as the onset of some kind of restricted chain rotation. The model of a cooperative flip-flop around the long-chain axis yields a quantitatively satisfying interpretation of both shape and time constants of the magnetization decays. The entire choline moiety appears to be in rapid motion, which can be understood as a rotation around the P—O bond to the glycerol backbone. (*c*) At the pretransition to the intermediate phase the hydrocarbon chains start a fast rotation regarded as free or weakly hindered with six equivalent positions. This concept is supported by x-ray results that indicate that the pretransition process is accompanied by a change in the chain lattice from orthorhombic to hexagonal.

In contrast to some other authors our dynamic model is based on rotational motions of the chains rather than on rotational and lateral diffusion of the entire molecule. We sum up the main arguments that support our model in comparison with molecular diffusion. In our opinion the idea of rotational chain motion is favored by the existence of a two-dimensional chain lattice, i.e., orthorhombic in the gel and hexagonal in the intermediate phase.

In the  $L_\beta$  phase the orthorhombic lattice and the chain tilt restrict the pathways of lateral diffusion as the molecule has to be deformed and the local tilt changed at almost every diffusion step. Therefore, it is not surprising that the lateral-diffusion coefficient of the order of  $10^{-11} \text{ cm}^2/\text{s}$  found for the  $L_\beta$  phase by Smith and McConnell (49) is by far too small to explain the observed reduction of the proton second moment at the subtransition. The short

correlation times found in our  $^{13}\text{C}$  study (22) indicate, however, that there is molecular motion in the  $L_\beta$  phase accessible to the NMR time scale. A correlated rotational chain hopping between the two preferential orthorhombic chain positions (Fig. 5) appears to be the most favored molecular motion in the  $L_\beta$  phase. Although we do not exclude lateral molecular diffusion in the hexagonal lattice of the  $P_\beta$  phase, we regard free chain rotation as the significant motional change occurring at the pretransition from  $L_\beta$  to  $P_\beta$ . This view is supported by various arguments. The diffusion rate as measured by Smith and McConnell (49) does not change discontinuously at the pretransition but increases continuously with temperature. The hexagonal lattice in the  $P_\beta$  phase indicates a cylindrical chain symmetry that is most effectively generated by free rotation of the chains around their long axes. Thus, the large discontinuous change of the motional correlation time reported in the preceding paper (22) is consistently interpreted as a change of the rotational motion of chains. In addition, our model is consistent with the absence of drastic effects of the pretransition on the second moments of the  $^{13}\text{C}$ -,  $^1\text{H}$ -, and  $^2\text{H}$ -NMR lines (21–24).

Interesting features of the subtransition are the extremely slow kinetics and its hysteresis. A plausible interpretation for the time dependence of the transition could be the building up new crystalline arrangements. The striking time-independent hysteresis indicates the existence of metastable crystalline states over a temperature range of 11 K. A further question possibly related to the preceding ones concerns the molecular cause of the subtransition. One aspect deserving consideration is the interaction of the monolayers at the ends of the hydrocarbon chains.  $^{13}\text{C}$ -NMR spectra with resolved terminal methyl groups might yield more information about this point. On the other hand, we have shown that the choline head group ceases its rotation below the subtransition. It was found in the preceding study (22) that at the pretransition the  $^{13}\text{C}$ - $^1\text{H}$  cross-polarization rate in the head-group moiety becomes liquidlike. These observations suggest that both low temperature transitions are linked to changes in the head-group arrangement.

The authors wish to thank Professor W. Helfrich for many helpful discussions.

This work was supported by the Deutsche Forschungsgemeinschaft. Experimental setup was provided by the Sonderforschungsbereich.

Received for publication 1 April 1982 and in final form 23 December 1982.

## REFERENCES

1. Tardieu, A., V. Luzzati, and F. C. Reman. 1973. Structure and polymorphism of the hydrocarbon chains of lipids: A study of lecithin-water phases. *J. Mol. Biol.* 75:711–733.
2. Janiak, M. J., D. M. Small, and G. G. Shipley. 1976. Nature of the thermal pretransition of synthetic phospholipids: Dimyristoyl- and dipalmitoyllecithin. *Biochemistry*. 15:4575–4580.
3. Rand, R. P., D. Chapman, and K. Larsson. 1975. Tilted hydrocarbon chains of dipalmitoyl lecithin become perpendicular to the bilayer before melting. *Biophys. J.* 15:1117–1124.
4. Büldt, G., H. U. Gally, A. Seelig, J. Seelig, and G. Zaccai. 1978. Neutron diffraction studies on selectively deuterated phospholipid bilayers. *Nature (Lond.)*. 271:182–184.
5. Gebhardt, C., H. Gruler, and E. Sackmann. 1977. On domain structure and local curvature in lipid bilayers and biological membranes. *Z. Naturforsch. Sect. C. Biosci.* 32:581–596.
6. Gaber, B. P., and W. L. Peticolas. 1977. On the quantitative interpretation of biomembrane structure by Raman spectroscopy. *Biochim. Biophys. Acta*. 465:260–274.
7. Yellin, N., and I. W. Levin. 1977. Hydrocarbon chain disorder in lipid bilayers. Temperature dependent Raman spectra of 1,2-diacyl phosphatidylcholine-water gels. *Biochim. Biophys. Acta*. 489:177–190.
8. Luna, E. J., and H. M. McConnell. 1977. The intermediate monoclinic phase of phosphatidylcholines. *Biochim. Biophys. Acta*. 466:381–392.
9. Seelig, A., and J. Seelig. 1974. The dynamic structure of fatty acyl chains in a phospholipid bilayer measured by deuterium magnetic resonance. *Biochemistry*. 13:4839–4845.
10. Kohler, S. J., and M. P. Klein. 1977. Orientation and dynamics of phospholipid head groups in bilayers and membranes determined from  $^{31}\text{P}$  nuclear magnetic resonance chemical shielding tensors. *Biochemistry*. 16:519–526.
11. Bloom, M., E. E. Burnell, A. L. MacKay, C. P. Nichol, M. I. Valic, and G. Weeks. 1978. Fatty acyl chain order in lecithin model membranes determined from proton magnetic resonance. *Biochemistry*. 17:5750–5762.
12. Cullis, P. R. 1976. Lateral diffusion rates of phosphatidylcholine in vesicle membranes: effects of cholesterol and hydrocarbon phase transitions. *FEBS (Fed. Eur. Biochem. Soc.) Lett.* 70:223–228.
13. Kimura, H., and H. Nakano. 1981. Successive phase transitions in lipid membranes. *Mol. Cryst. Liq. Cryst.* 68:289–299.
14. Brady, G. W., and D. B. Fein. 1977. An analysis of the x-ray interchain peak profile in dipalmitoylglycerophosphocholine. *Biochim. Biophys. Acta*. 464:249–259.
15. Inoko, Y., and T. Mitsui. 1978. Structural parameters of dipalmitoyl phosphatidylcholine lamellar phases and bilayer phase transitions. *J. Phys. Soc. Jpn.* 44:1918–1924.
16. Hentschel, M., R. Hosemann, and W. Helfrich. 1980. Direct x-ray study of the molecular tilt in dipalmitoyl lecithin bilayers. *Z. Naturforsch. A*. 35:643–644.
17. Hentschel, M. 1981. Ph.D. dissertation. Röntgenstrukturuntersuchungen von orientierten Lecithin-Vielschichtsystemen. Freie Universität Berlin.
18. Janiak, M. J., D. M. Small, and G. G. Shipley. 1979. Temperature and compositional dependence of the structure of hydrated dimyristoyl lecithin. *J. Biol. Chem.* 254:6068–6078.
19. Copeland, B. R., and H. M. McConnell. 1980. The rippled structure in bilayer membranes of phosphatidylcholine and binary mixtures of phosphatidylcholine and cholesterol. *Biochim. Biophys. Acta*. 599:95–109.
20. Pink, D. A., T. J. Green, and D. Chapman. 1980. Raman scattering in bilayers of saturated phosphatidylcholines. Experiment and theory. *Biochemistry*. 19:349–356.
21. Trahms, L., and E. Boroske. 1979. Pulse NMR study of phase transitions in dipalmitoyl phosphatidylcholine multilayer systems. *Biochim. Biophys. Acta*. 552:189–193.
22. Boroske, E., and L. Trahms. 1983. A  $^1\text{H}$  and  $^{13}\text{C}$  NMR study of motional changes of dipalmitoyl lecithin associated with the pretransition. *Biophys. J.* 42:275–283.
23. Davis, J. H. 1979. Deuterium magnetic resonance study of the gel and liquid crystalline phases of dipalmitoyl phosphatidylcholine. *Biophys. J.* 27:339–358.
24. MacKay, A. L. 1981. A proton NMR moment study of the gel and



- liquid-crystalline phases of dipalmitoyl phosphatidylcholine. *Biophys. J.* 35:301–313.
25. Cameron, D. G., H. L. Casal, E. F. Gudgin, and H. H. Mantsch. 1980. The gel phase of dipalmitoyl phosphatidylcholine—an infrared characterization of the acyl chain packing. *Biochim. Biophys. Acta.* 596:463–467.
  26. Cameron, D. G., H. L. Casal, and H. H. Mantsch. 1980. Characterization of the pretransition in 1,2-dipalmitoyl-sn-glycero-3-phosphocholine by Fourier transform infrared spectroscopy. *Biochemistry.* 19:3665–3672.
  27. Cameron, D. G., H. L. Casal, H. H. Mantsch, Y. Boulanger, and I. C. P. Smith. 1981. The thermotropic behavior of dipalmitoyl phosphatidylcholine bilayers. A Fourier transform infrared study of specifically labeled lipids. *Biophys. J.* 35:1–16.
  28. Chen, S. C., J. M. Sturtevant, and B. J. Gaffney. 1980. Scanning calorimetric evidence for a third phase transition in phosphatidylcholine bilayers. *Proc. Natl. Acad. Sci. USA.* 77:5060–5063.
  29. Földner, H. H. 1981. Characterization of a third phase transition in multilamellar dipalmitoyllecithin liposomes. *Biochemistry.* 20:5707–5710.
  30. Ruocco, M. H., and G. G. Shipley. 1982. Characterization of the subtransition of hydrated dipalmitoylphosphatidylcholine bilayers. X-ray diffraction study. *Biochim. Biophys. Acta* 684:59–66.
  31. Goldman, M. 1970. Spin temperature and Nuclear Magnetic Resonance in solids. W. Marshall and D. H. Wilkinson, editors. Oxford University Press, London.
  32. Abragam, A. 1961. Principles of Nuclear Magnetism. N. F. Mott, E. C. Bullard, and D. H. Wilkinson, editors. Oxford University Press, London.
  33. Bloom, M., E. E. Burnell, S. R. W. Roeder, and M. I. Valic. 1977. Nuclear magnetic resonance line shapes in lyotropic liquid crystals and related systems. *J. Chem. Phys.* 66:3012–3019.
  34. Boden, N., Y. K. Levine, D. Lightowers, and R. T. Squires. 1975. NMR dipolar echoes in solids containing spin  $-1/2$  pairs. *Mol. Phys.* 29:1877–1891.
  35. Boden, N., Y. K. Levine, D. Lightowers, and R. T. Squires. 1975. NMR dipolar echoes in liquid crystals. *Chem. Phys. Lett.* 31:511–515.
  36. Boden, N., Y. K. Levine, D. Lightowers, and R. T. Squires. 1975. Internal molecular disorder in the nematic and smectic phases of thermotropic liquid crystals studies by NMR SPDE experiments. *Chem. Phys. Lett.* 34:63–68.
  37. Boden, N., P. Jackson, Y. K. Levine, and A. J. I. Ward. 1976. Intramolecular disorder and its relation to mesophase structure in lyotropic liquid crystals. *Chem. Phys. Lett.* 37:100–105.
  38. Trahms, L. 1982. Ph.D. dissertation. Untersuchung der molekularen Dynamik in Lecithin-Doppelschichten mit der Methode der NMR. Freie Universität Berlin.
  39. Büldt, G., and R. Wohlgemuth. 1981. The headgroup conformation of phospholipids in membranes. *J. Membr. Biol.* 58:81–100.
  40. Seelig, J., H.-U. Gally, and R. Wohlgemuth. 1977. Orientation and flexibility of the choline head group in phosphatidylcholine bilayers. *Biochim. Biophys. Acta.* 467:109–119.
  41. Seelig, J. 1978.  $^{31}\text{P}$  nuclear magnetic resonance and the head group structure of phospholipids in membranes. *Biochim. Biophys. Acta.* 515:105–140.
  42. Seelig, J., and W. Niederberger. 1974. Two pictures of a lipid bilayer. A comparison between deuterium label and spin-label experiments. *Biochemistry.* 13:1585–1588.
  43. Brown, M. R., J. Seelig, and U. Haeberlen. 1979. Structural dynamics in phospholipid bilayers from deuterium spin-lattice relaxation time measurements. *J. Chem. Phys.* 70:5045–5053.
  44. Boroske, E., L. Mayas, and K. Möbius. 1979. A molecular structure study of partially deuterated succinic acid by  $^1\text{H}$  and  $^2\text{H}$  distant ENDOR. *J. Magn. Reson.* 35:231–246.
  45. Andrew, E. R. 1950. Molecular motion in certain solid hydrocarbons. *J. Chem. Phys.* 18:607–618.
  46. Lawson, K. D., and T. Flautt. 1965. Nuclear magnetic resonance absorption in anhydrous sodium soaps. *J. Phys. Chem.* 69:4256–4268.
  47. Jeffrey, K. R., T. C. Wong, E. E. Burnell, M. J. Thompson, T. P. Higgs, and N. R. Chapman. 1979. Molecular motion in the lyotropic liquid crystal system containing potassium palmitate: a study of proton spin-lattice relaxation times. *J. Magn. Reson.* 36:151–171.
  48. Peters, A., and R. Kimmich. 1978. The heterogeneous solubility of oxygen in aqueous lecithin dispersions and its relation to chain mobility: a NMR relaxation and wideline study. *Biophys. Struct. Mechan.* 4:67–85.
  49. Smith, B. A., and H. M. McConnell. 1978. Determination of molecular motion in membranes using periodic pattern photo-bleaching. *Proc. Natl. Acad. Sci. USA.* 75:2759–2763.